EPJ Web of Conferences **49**, 12004 (2013)
DOI: 10.1051/epjconf/20134912004

Search for SM Higgs decaying to two W bosons at CMS

Phillip R. Dudero[1,2,a]

[1] *CMS Collaboration*
[2] *Texas Tech University*

Abstract. Updated results of searches for the standard model Higgs boson decaying to two W bosons in pp collisions at $\sqrt{s}$=8 TeV are reported. The fully leptonic (WW→ $2\ell 2\nu$) and semileptonic (WW→ $\ell\nu jj$) final state searches are presented. The event sample corresponds to an integrated luminosity of 12 fb^{-1}collected by the CMS detector in 2012. The 2011 results obtained at $\sqrt{s}$=7 TeV for an integrated luminosity of 5 fb^{-1}are added to the analysis. The leptonic channel observes an excess at M=125 GeV with a significance of 3.1σ. Upper limits are derived for the remainder of the mass range up to 600 GeV. Results are also presented for Higgs production in association with a W boson, leading to the $3\ell 3\nu$ final state using 5 fb^{-1}collected at $\sqrt{s}$=8 TeV combined with data collected in 2011.

1 Introduction

A primary goal of the Large Hadron Collider (LHC) [1] experiments is to study the mechanism of electroweak symmetry breaking, which provides mass to the W and Z bosons while the photon remains massless. The Standard Model (SM) postulates the mechanism of electroweak symmetry breaking with the Higgs field as a possible explanation [2–4]. A consequence of the Higgs field would be existence of the spin-zero Higgs boson (H) with quantum numbers of the vacuum $J^{PC} = 0^{++}$. Indirect measurements [5] and direct searches at TeVatron [6] suggest that the mass of the SM Higgs boson would most likely fall below 200 GeV, where a new resonance has been observed around 125 GeV by both ATLAS and CMS collaborations [7, 8].

Here we present the results of three searches for a Standard Model Higgs decaying to two W bosons, using data corresponding to an integrated luminosity of 12 fb^{-1}collected with the CMS detector [9] in pp collisions at $\sqrt{s}$ = 8 TeV at the CERN LHC in 2012. The results are then combined with those obtained from 5 fb^{-1}of pp collisions collected in 2011 at $\sqrt{s}$ = 7 TeV.

2 Physics objects

The search strategy for all channels presented herein require the reconstruction of detector objects, namely electron and muon candidates, jets and missing transverse energy, or $E_{\mathrm{T}}^{\mathrm{miss}}$.

Muons are required to be isolated to distinguish between muon candidates from W-boson decays and those from QCD background processes, which are usually in or near jets. For each muon candidate, the scalar sum of the transverse energy of all particles compatible with originating from the primary vertex is reconstructed in cones of several widths around the muon direction. Electron candidates are identified using a multivariate approach based on variables similar to those described in [10] and exploiting information from the tracker, the ECAL, and the combination of these two detectors. Electrons are required to be isolated by applying a threshold on the sum of the transverse energy of the particles which are reconstructed in a cone around them. For both electrons and muons a correction is applied to account for the contribution to the energy in the isolation cone from the pile-up using the measured median energy density in the event. They are required to originate from the primary vertex of the event.

Jets are reconstructed using the anti-k_{T} clustering algorithm [11] with distance parameter $\Delta R = 0.5$. A similar correction as for the lepton isolation is applied to account for the contribution to the jet energy from the pile-up. Jet energy corrections are applied as a function of the jet E_{T} and η. A selection is applied to separate jets from the primary interaction from those reconstructed due to energy deposits associated with pile-up, based on the differences in the jet shapes, in the relative multiplicity of charged and neutral components and in the different fraction of transverse momentum which is carried by the hardest components. Within the tracker acceptance the jet tracks are also required to be compatible with the primary vertex. Events are classified according to the number of selected jets with $E_{\mathrm{T}} > 30$ GeV and $|\eta| < 4.7$.

In addition to high momentum isolated leptons and minimal jet activity missing transverse momentum is present in signal events due to $\mathrm{W} \to \ell\nu$ decays. For the $\mathrm{W^+W^-} \to \ell\nu\ell\nu$ final state with same-flavor leptons, a large background comes from Drell-Yan process, where no real $E_{\mathrm{T}}^{\mathrm{miss}}$ is present. In this case a *projected* $E_{\mathrm{T}}^{\mathrm{miss}}$ variable is

[a] e-mail: pdudero@ttu.edu

employed. It is equal to the component of $E_{\mathrm{T}}^{\mathrm{miss}}$ transverse to the nearest lepton if the difference in azimuth between this lepton and the $E_{\mathrm{T}}^{\mathrm{miss}}$ vector is less than $\pi/2$. If there is no lepton within $\pi/2$ of the direction of $E_{\mathrm{T}}^{\mathrm{miss}}$ in azimuth, $E_{\mathrm{T}}^{\mathrm{miss}}$ is used directly. Since the *projected* $E_{\mathrm{T}}^{\mathrm{miss}}$ resolution is degraded by pile-up, the minimum of two $E_{\mathrm{T}}^{\mathrm{miss}}$ observables is used: the first includes all reconstructed particles in the event, while the second uses only the charged particles associated with the primary vertex. In the semi-leptonic final state, since the main background arises from associated W and jets production with real $E_{\mathrm{T}}^{\mathrm{miss}}$, no projection is needed.

3 H→WW→ $\ell\nu\ell\nu$ search [12]

In this search channel, two gluons or two vector bosons radiated from quarks fuse to produce the Higgs boson, which then decays through two W bosons to a final state signature with two isolated, oppositely charged, high-p_{T} leptons (electrons or muons) and large $E_{\mathrm{T}}^{\mathrm{miss}}$due to the undetected neutrinos. The events are selected by triggers that require the presence of one or two high-p_{T} electrons or muons. Two oppositely charged leptons are required to be reconstructed with p_{T}>20 GeV for the leading lepton and p_{T}>10 GeV for the trailing lepton. Only electrons (muons) with $|\eta|$ <2.5 (2.4) are considered in the analysis. The *projected* $E_{\mathrm{T}}^{\mathrm{miss}}$is required to exceed 20 GeV.

Events are classified according to the number of selected jets with E_t>30 GeV and $|\eta|$ <4.7 into three mutually exclusive categories, which are characterized by different signal yields and signal-to-background ratios. In the following we call these the 0-jet, 1-jet and 2-jet samples. Events with more than two jets are not considered. Furthermore, the search strategy splits signal candidates into same-flavor lepton category ($e^+e^-, \mu^+\mu^-$) and different-flavor lepton category ($e^{+-}\mu^{-+}$). The bulk of the signal arises through direct W decays to electrons or muons, while a small contribution proceeding through an intermediate τ-lepton decays is implicitly included. More details about the analysis can be found in Ref. [8].

The various backgrounds are suppressed using techniques described in [8]. Top-quark backgrounds are controlled with a top-tagging technique based on soft-muon and b-jet tagging [13]. A minimum dilepton transverse momentum ${p_{\mathrm{T}}}^{\ell\ell}$ of 45 GeV is required to reduce the W+jets background. Rejection of a third lepton passing the identification and isolation requirements reduces both WZ and Wγ backgrounds, where in the latter case a photon is misidentified as an electron. The background from low mass resonances is rejected by requiring a dilepton mass ($m_{\ell\ell}$) greater than 12 GeV. The Drell-Yan process produces same-flavor lepton pairs ($e^+e^-, \mu^+\mu^-$), therefore a few additional requirements are applied in the same-flavor final states. First, the resonant component of the Drell-Yan production is rejected by requiring a dilepton mass outside a 30 GeV window centered on the Z mass. Then, the remaining off-peak contribution is suppressed by requiring the minimum of the two *projected* $E_{\mathrm{T}}^{\mathrm{miss}}$variables to be greater than 45 GeV. For events with two jets, the dominant source of fake $E_{\mathrm{T}}^{\mathrm{miss}}$is the mismeasurement of the hadronic recoil and the optimal performance is obtained by simply requiring $E_{\mathrm{T}}^{\mathrm{miss}}$> 45 GeV. Finally, the momenta of the dilepton system and of the most energetic jet must not be back-to-back in the transverse plane. These selections effectively reduce the Drell-Yan background by three orders of magnitude, while rejecting less than 50% of the signal.

These requirements comprise a set of "preselection" criteria; the resulting sample is dominated by non-resonant WW events. To enhance the sensitivity to a Higgs boson signal, two subsequent approaches are taken: a cut-based approach for all categories, optimized by category, and a two-dimensional shape analysis technique specifically for the different-flavor final state, 0-jet and 1-jet categories. This second analysis is more sensitive to the presence of a Higgs boson and is used as a baseline for the final results.

The cut-based approach employs additional requirements on $p_{\mathrm{T}}^{\ell,\mathrm{max}}$, $p_{\mathrm{T}}^{\ell,\mathrm{min}}$, $m_{\ell\ell}$, $\Delta\phi_{\ell\ell}$ and the transverse mass M_{T}, defined as $\sqrt{2p_{\mathrm{T}}^{\ell\ell}E_{\mathrm{T}}^{\mathrm{miss}}(1-\cos\Delta\phi_{E_{\mathrm{T}}^{\mathrm{miss}}\ell\ell})}$, where $\Delta\phi_{E_{\mathrm{T}}^{\mathrm{miss}}\ell\ell}$ is the difference in azimuth between $E_{\mathrm{T}}^{\mathrm{miss}}$ and the transverse momentum of the dilepton system. The 2-jet category is optimized for the VBF production mode.

The backgrounds that remain after applying the final selections are estimated by a combination of techniques, which are described in [8]. The $\mathrm{t\bar{t}}$ background is estimated by extrapolation from the observed number of events with the b-tagging cut inverted. The Drell-Yan background measurement is based on extrapolation from the observed number of e^+e^- and $\mu^+\mu^-$ events with the Z-veto cut inverted. The background W+jets and QCD multi-jet events is derived from measuring the number of events with one lepton passing a loose cut on isolation. The probabilities for such loosely-isolated fake leptons to pass tight isolation cut are measured in data using multi-jets events. The non-resonant WW contribution is taken from simulation. The number of events predicted by these estimations versus those observed in data for m_{H}=125 GeV is shown in Table 1. An excess of events with respect to the total background prediction is observed in most final states for low Higgs mass selections. A two-dimensional shape analysis using two independent variables, M_{T} and $m_{\ell\ell}$, has also been developed for the different-flavor final state. In addition to the preselection, a loose set of requirements are applied to M_{T}, $m_{\ell\ell}$, and p_{T} of the leading lepton. The plane is divided into 80 bins, the size of which is optimized to avoid having empty bins for the overall background contribution for the present Monte Carlo statistics, while still keeping enough cells to differentiate the signal shape from the background shape. All bins enter a binned likelihood fit of the data to the signal and background hypotheses in this two-dimensional shape analysis.

The M_{T}-$m_{\ell\ell}$two-dimensional distributions for the m_H = 125 GeV Higgs signal hypothesis of data minus background after the CLs fit in a smaller range, along with a projection of M_{T} in the signal-like region, are shown in Figure 1 for the 0-jet sample. An excess of events is observed in the signal-like region. The m_H = 125 GeV Higgs signal hypothesis provides a good description of

Table 1. Observed number of events, background estimates and signal predictions for m_H=125 GeV for an integrated luminosity of 12 fb^{-1} after applying the cut-based final selection requirements. The combined statistical, experimental, and theoretical systematic uncertainties are reported. The $Z/\gamma^* \to \ell^+\ell^-$ process includes the dimuon, dielectron and ditau final state.

Final State	H $\to W^+W^-$	pp $\to W^+W^-$	WZ + ZZ $+Z/\gamma^* \to \ell^+\ell^-$	Top	W + jets	$W\gamma^{(*)}$	all bkg.	data
$e\mu$ 0-jet	58 ± 12	203 ± 19	6.6 ± 0.6	11.0 ± 2.5	44 ± 16	25.6 ± 9.5	291 ± 27	349
$e\mu$ 1-jet	27.3 ± 8.0	47.9 ± 7.8	6.5 ± 0.7	49.5 ± 3.3	22.4 ± 8.6	7.1 ± 3.4	134 ± 13	160
$e\mu$ 2-jet	2.8 ± 0.4	0.9 ± 0.5	0.1 ± 0.0	1.5 ± 0.5	0.3 ± 0.2	0.1 ± 0.1	2.9 ± 0.8	2
$ee/\mu\mu$ 0-jet	37.0 ± 8.0	140 ± 13	59 ± 18	5.2 ± 1.3	30 ± 11	6.7 ± 2.8	241 ± 25	266
$ee/\mu\mu$ 1-jet	11.8 ± 3.4	24.8 ± 4.1	13.1 ± 3.5	26.7 ± 2.3	6.5 ± 2.8	2.0 ± 1.2	73.0 ± 6.6	92
$ee/\mu\mu$ 2-jet	1.5 ± 0.2	0.5 ± 0.3	4.4 ± 1.3	0.7 ± 0.2	0.8 ± 0.5	0.1 ± 0.1	6.5 ± 1.5	11

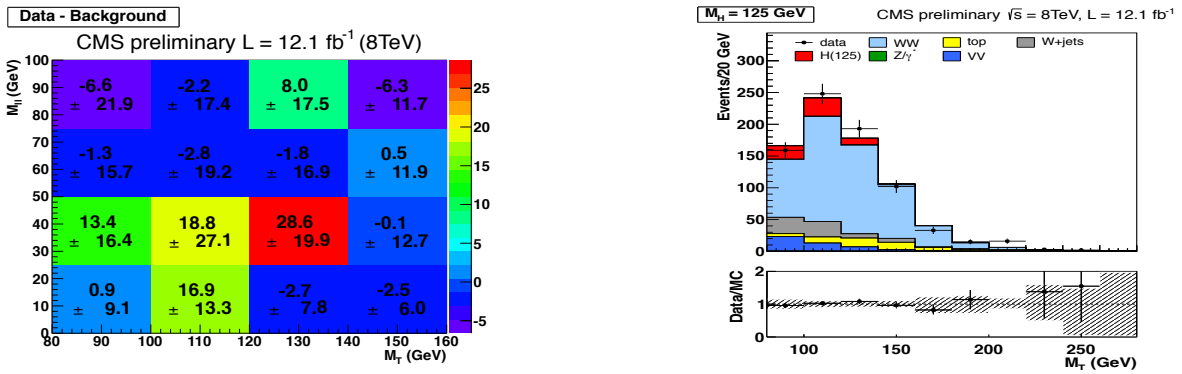

Figure 1. (left) Two-dimensional distribution, shown in a smaller range, in the 0-jet bin, of data minus background after the CLs fit for the m_H = 125 GeV Higgs signal hypothesis for the $2\ell 2\nu$ final state. (right) The projection of M_T for the more signal-like region $m_{\ell\ell}$< 50 GeV.

the data within the statistical and systematic uncertainties. The 95% observed and expected median C.L. upper limits computed with the CL_s method are shown in Figure 2. We combine the shape-based analysis in the different-flavor final state, 0-jet and 1-jet categories, with the cut-based analysis in all other categories, and also with the analysis performed at 7 TeV. The bands represent the 1σ and 2σ probability intervals around the expected limit. The a posteriori probability intervals on the cross section are constrained by the a priori minimal assumption that the signal and background cross sections are positive definite. The combination of the results from the 8 TeV data using the shape analysis, and the analysis performed at 7 TeV, excludes a Higgs boson in the mass in the range 128–600 GeV at 95% CL. The expected exclusion range for the background only hypothesis is 118–565 GeV. An excess of events is observed for hypothetical low Higgs boson masses, which makes the observed limits weaker than the expected ones. Due to the poor mass resolution of this channel the excess extends over a large mass range.

The expected and observed significance and best fit value of σ/σ_{SM} for a SM Higgs with a mass of 125 GeV are summarized in Table 2. The significance of the excess with respect to the background only hypothesis at this mass is 3.1 standard deviations for the 7+8 TeV shape-based analysis. The best fit value of σ/σ_{SM} in the mass range $110 < m_H < 600$ GeV is shown in Figure 2.

Table 2. Expected and observed significance and best fit value of σ/σ_{SM} for a SM Higgs with a mass of 125 GeV for the $2\ell 2\nu$ final state. Results are reported for the cut-based approach using the 8 TeV data only, for the shape-based approach using the 8 TeV data only and for the combined 8 TeV shape-based analysis together with the analysis performed at 7 TeV.

expected/observed significance		
8 TeV cut-based	8 TeV shape-based	7+8 TeV shape-based
2.4/1.7	3.7/2.9	4.1/3.1
best fit value		
8 TeV cut-based	8 TeV shape-based	7+8 TeV shape-based
0.80 ± 0.45	0.77 ± 0.28	0.74 ± 0.25

4 H→WW→ $\ell\nu qq$ search [14]

The advantage of this channel over the fully leptonic final state is that it has a larger branching fraction and a reconstructable Higgs mass peak [70]. Unfortunately this is more than offset by the expense of a large W+jets back-

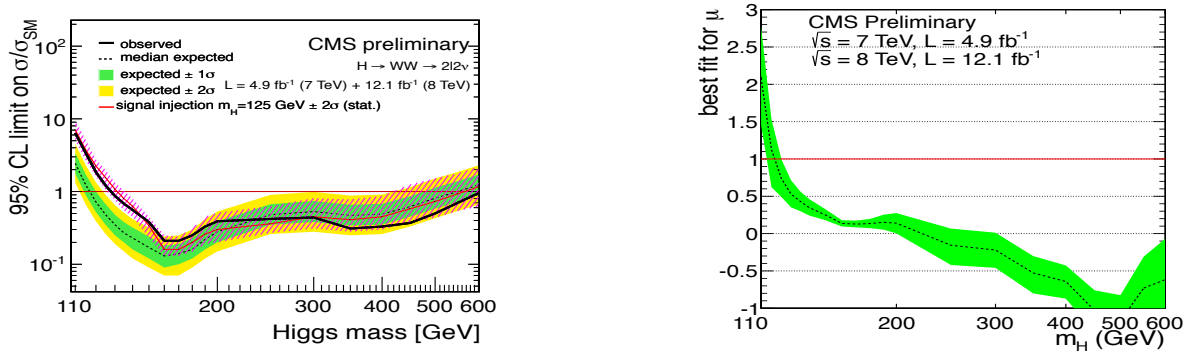

Figure 2. (left) Expected and observed 95% CL upper limits on the cross section times branching fraction, $\sigma_H \times \mathrm{BR}(H \to WW \to \ell\nu\ell\nu)$, relative to the SM Higgs expectation, for the combined 8 TeV shape-based analysis in the 0-jet and 1-jet categories together with the cut-based analysis in all other categories and the analysis performed at 7 TeV. (right) The best fit value of σ/σ_{SM}.

ground; the level to which this background is controlled determines the sensitivity of the analysis.

Object reconstruction proceeds as described above. The combination of the two highest p_{T} jets within $|\eta| < 2.5$ is chosen as the hadronic W candidate. The events with the incorrect dijet combination comprise a broad non-peaking background in the WW mass spectrum. The leptonic W candidate is reconstructed from the lepton plus $E_{\mathrm{T}}^{\mathrm{miss}}$system. We require $E_{\mathrm{T}}^{\mathrm{miss}}$>25(30) GeV for each event in the muon (electron) data. In addition, the unmeasurable longitudinal component of the neutrino momentum is reconstructed by requiring the lepton-neutrino pair to have the invariant mass of a W boson. The ambiguity in the second-order equation is resolved by taking the solution that yields the smallest $|p_{\mathrm{z}}|$ value.

The transverse mass of the leptonic W candidate is defined as $M_{\mathrm{T}} \equiv \sqrt{2\, p_{\mathrm{T}}^{l}\, E_{\mathrm{T}}^{\mathrm{miss}}\, (1 - \cos(\phi_l - \phi_{E_{\mathrm{T}}^{\mathrm{miss}}}))}$, where ϕ_l and $\phi_{E_{\mathrm{T}}^{\mathrm{miss}}}$ are the azimuthal angles of the lepton and $E_{\mathrm{T}}^{\mathrm{miss}}$, respectively. To reduce the background from processes that do not contain $\mathrm{W} \to \ell\nu$ decays, the transverse mass M_{T} is required to be larger than 30 GeV.

To exploit the differences in kinematics between signal and background, a likelihood discriminant is constructed that incorporates a set of variables that best distinguishes the Higgs signal from the W+jets background. These variables comprise five angles between the Higgs decay products that fully describe the Higgs production kinematics [15], the p_{T} and rapidity of the WW system, and the lepton charge. The likelihood discriminant is optimized for each simulated Higgs mass hypothesis, for each lepton flavor (e, μ) and for each jet multiplicity (2 jets, 3 jets) independently. Events are retained if they survive a simple selection on the likelihood discriminant, chosen on the basis of the expected limit for the Higgs extraction as the figure of merit.

The remainder of the analysis in this channel consists of a two-body fit of the invariant mass m_{jj} of the dijet system, which is the hadronic W candidate, to extract the normalization of background components, and a construction of the shape of the four-body of invariant mass m_{WW} distribution of the $\ell\nu jj$ system, which is the primary observable used to set exclusion limits.

The background normalization in the signal region is extracted, for each Higgs mass hypotheses independently, with an unbinned maximum likelihood fit to the m_{jj} distribution. The signal region corresponding to the W mass window, 65 GeV $< m_{jj} <$ 95 GeV, is excluded from the fit. The shape of the W+jets background is derived from simulation, and the overall normalization is allowed to vary in the fit. The WW/WZ, $\mathrm{t\bar{t}}$, single top, and Drell-Yan+jets shapes are based on simulation and their normalization are constrained to the theoretical predictions, within the corresponding uncertainties. The multi-jet background shape is derived from data by relaxing lepton isolation and identification requirements. Its contribution to the total number of events is evaluated from a separate two-component likelihood fit to the W transverse mass distribution. For muons, the multijet fraction is negligible, while for electrons it is several percent depending on the jet multiplicity in the event. The multijet contribution is constrained to these values in the m_{jj} fit within uncertainties. The uncertainties in the total background normalization obtained from the fit are propagated to the limit calculation as a systematic uncertainty.

The four-body mass shape of the W+jets contribution is extracted from data as a linear combination of the shape measured in two signal-free regions, namely an upper sideband (SBH, 95 GeV $< m_{jj} <$ 115 GeV) and a lower sideband (SBL, 55 GeV $< m_{jj} <$ 65 GeV). Because of the low statistics, the shapes are regularized by means of an exponential fit (solid curve). The four-body mass shape for multijet background events is obtained from the same data sample as described for the m_{jj} fit. All other background categories use the $m_{\ell\nu jj}$ shape predicted by their respective Monte Carlo samples. The largest source of systematic uncertainty is due to $m_{\ell\nu jj}$-shape uncertainty of the W+jets background. The only other uncertainty assigned to background is the normalization uncertainty from the m_{jj} fit. Both of these uncertainties are estimated from data. All other systematic uncertainties are applied to sig-

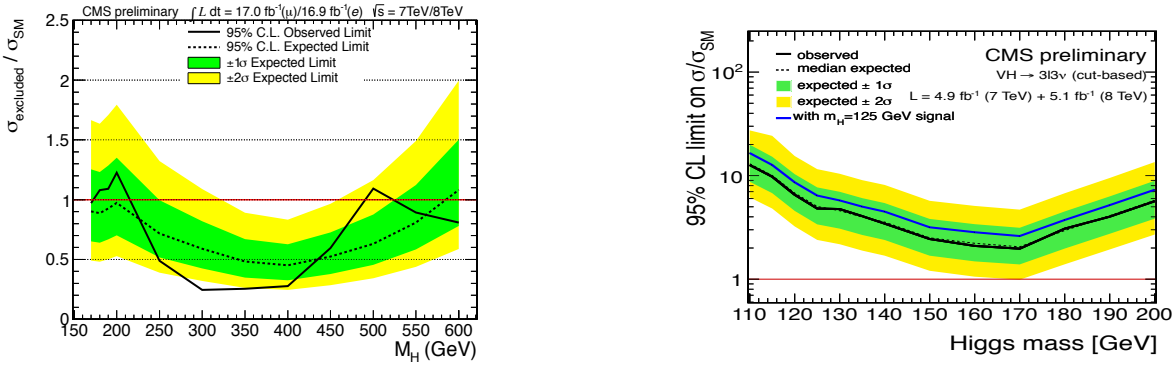

Figure 3. Observed (solid) and expected (dashed) 95% CL upper limit on the ratio of the production cross section to the SM expectation for the Higgs boson in the semileptonic final state (left) and the $3\ell 3\nu$ final state (right). The limits combine data from both 7 TeV and 8 TeV collisions.

nal processes. The dominant signal uncertainties include theoretical uncertainties for the cross section (14-19% for gluon fusion) and exclusive jet binning effects on scale (4-28%), as well as the efficiency of the likelihood selection (10%). The latter effect is computed by taking the relative difference in efficiency between data and simulation using a control sample of top pair events in data. These events are good proxies for the signal, since in both cases the primary production mechanism is gluon-gluon fusion, and the semi-leptonic final states contain decays of two W bosons.

Upper limits on the SM Higgs boson production cross section have been calculated. We present 95% exclusion limits on the ratio of the production cross section for the Higgs boson compared to the SM expectation in Figure 3. Combining with 7 TeV results [16], we exclude the SM Higgs boson in the mass ranges 215–490 GeV and 525–600 GeV at 95% confidence level, while the median expected one becomes 170–585 GeV.

5 WH→WWW→ $3\ell 3\nu$ search [17]

This channel involves the production of a Higgs boson in association with a W Boson. The Higgs boson subsequently decays into a pair of W bosons, WH(→WW). The final state consists of three leptons and three neutrinos arising from each of the W→ $\ell\nu$ decays. The cross section of this process exhibits a maximum for Higgs boson masses near twice the W mass, due to the combined behavior of production cross section and the branching fraction for H → W^+W^-. The search is sensitive to the WH(→ $\tau\tau$) process via τ leptonic decays, and therefore was also considered as part of the signal component. The data sample corresponds to an integrated luminosity of 4.9±0.1 fb^{-1}at $\sqrt{s}$ = 7 TeV and 5.1±0.2 fb^{-1}at $\sqrt{s}$ = 8 TeV. We follow a cut-based mass independent selection, optimized for mH = 125 GeV. Many of the same techniques described for the $2\ell 2\nu$ final state were used here as well. In total, four categories are considered: the two center-of-mass energies and the opposite-sign same-flavor (OSSF) and same-sign same-flavor (SSSF) final states. No significant excess of events is observed with respect to the background prediction, and 95% CL upper limits are calculated for the Higgs boson cross section with respect to the SM Higgs boson expectation. The expected and observed upper limits with 10 $fb^{-1}$of data are shown in Figure 5. The observed (expected) upper limit at the 95% CL is 4.8 (5.0) times larger than the SM expectation for m_H= 125 GeV.

References

[1] L. Evans and P. Bryant (eds.), JINST **3**, S08001 (2008)

[2] Englert, F. and Brout, R., Phys. Rev. Lett. **13**,321-322 (1964)

[3] Higgs, Peter W., Phys. Rev. Lett. **13**, 508-509 (1964)

[4] Guralnik, G. S. and Hagen, C. R. and Kibble, T. W. B.,Phys. Rev. Lett. **13**, 585-587 (1964)

[5] ALEPH, CDF, D0, DELPHI, L3, OPAL, SLD Collaborations, the LEP Electroweak Working Group, the Tevatron Electroweak Working Group, and the SLD electroweak and heavy flavour groups, CERN-PH-EP-2010-09, FERMILAB-TM-2480-PPD, SLAC-PUB-14301 (2010)

[6] CDF, D0, and the TEVNPHWG Working Group, arXiv:1103.3233 (2011)

[7] Aad, Georges *et. al.*, Phys.Lett. B **716**,1-20 (2012)

[8] Chatrchyan, Serguei *et. al.*, Phys.Lett. B **716**,30-61 (2012)

[9] CMS Collaboration, JINST **3**, S08004 (2008)

[10] CMS Collaboration, CMS-PAS-EGM-10-004 (2010)

[11] M. Cacciari and G. P. Salam and G. Soyez, JHEP, **04** 063 (2008)

[12] CMS Collaboration, CMS-PAS-HIG-12-042 (2012)

[13] CMS Collaboration, CMS-PAS-BTV-11-003 (2011)

[14] CMS Collaboration, CMS-PAS-HIG-12-046 (2012)

[15] Gao, Yanyan *et. al.*, Phys. Rev. D, **81** 075022 (2010)

[16] CMS Collaboration, CMS-PAS-HIG-12-003 (2012)

[17] CMS Collaboration, CMS-PAS-HIG-12-039 (2012)